High Order Shock Capturing Schemes — An Overview

Chi-Wang Shu

Division of Applied Mathematics

Brown University

Outline

- Introduction
- Brief comparison of several high order methods
- Examples of a few recent developments on high order methods
- Concluding remarks

Introduction

- We are interested in numerically solving hyperbolic conservation laws

$$u_t + f(u)_x + g(u)_y + h(u)_z = 0 \tag{1}$$

where $\xi_1 f'(u) + \xi_2 g'(u) + \xi_3 h'(u)$ is diagonalizable with real eigenvalues for any real $\xi = (\xi_1, \xi_2, \xi_3)$. The solution may have discontinuous solutions (shocks, contact discontinuities, etc.) even if the initial and boundary conditions are smooth.

- Selected list of applications:
  - Traffic flows
  - Computational fluid dynamics, especially high speed flows
  - Electro-magnetic waves, aeroacoustics
  - Astrophysics
  - Semiconductor device simulations
  - Certain problems in computational biology
  - . . .

In many applications, we often encounter the so-called convection dominated problems. i.e. the PDEs (1) with additional terms rather than zero on the right hand side, however these additional terms have a small coefficient.

- For example, a one dimensional convection dominated convection-diffusion equation is given by

$$u_t + f(u)_x = \varepsilon(a(u)u_x)_x$$

where $a(u) \geq 0$ and $0 < \varepsilon \ll 1$.

- A one dimensional convection dominated convection-dispersion equation is given by

$$u_t + f(u)_x = \varepsilon a(u)_{xxx}$$

where $a(u)$ is an arbitrary function and $0 < \varepsilon \ll 1$. For $f(u) = \alpha u + \beta u^2$ and $a(u) = u$ this is the famous Korteweg-de Vries (KdV) equation.

- Another good example is the compressible Navier-Stokes equation with high Reynolds numbers, which is the Euler equation plus a diffusion right hand side with a small coefficient $\frac{1}{Re}$ where Re is the Reynolds number.

For convection dominated problems, the main difficulty for the numerical solutions is the treatment of the convection terms.

Importance of high order methods for convection dominated problems:

- For smooth solutions, especially for time dependent problems with large time, high order methods are much more efficient than lower order ones to reach the same error tolerance. The smaller this tolerance, the longer the simulation time, the more efficient high order methods will be (Kreiss).

- For non-smooth or even discontinuous solutions of linear PDEs, such as the Maxwell equations in computational electro-magnetism and linearized Euler equations in aeroacoustics, it can be proved that a high order scheme is still high order accurate, measured in a suitable negative norm. Then a suitable post-processor can recover high order accuracy in a strong norm such as the L^2 norm (Mock and Lax, Majda, McDonough and Osher, Cockburn, Luskin, Shu and Süli, etc.).

- For non-smooth or even discontinuous solutions of nonlinear PDEs, such as the Euler equations of compressible gas dynamics:
  - A rigorous mathematical proof of the high order convergence in a suitable negative norm of high order schemes is not known.
  - It is also true that many of the unmodulated high order schemes such as the spectral method and high order compact schemes may become nonlinearly unstable when computing solutions containing strong discontinuities, rendering the computer codes to crash.

- However, there are still reasons to believe that high order accurate schemes, especially those modern high order accurate, “high resolution” schemes which have nonlinear mechanisms to control spurious oscillations, such as the WENO schemes, are suitable choices for solving nonlinear PDEs with discontinuous solutions, especially when the solutions contain both discontinuities and complicated smooth region structure.
- Lax (1978) argued that, for a nonlinear system, high order information is retained by a high order scheme and may be extracted by postprocessing. In fact, Lax’s argument indicates that more high order information is retained in high order solutions of nonlinear systems than of linear ones, since in the nonlinear case the solution operator is contractive.

Brief comparison of several high order methods

If the solution of the PDE is smooth:

- The spectral method is the most efficient numerical method. The error is smaller than $O(N^{-k})$ for any finite k, if the solution is C^{k+1}. If the solution is analytic, then the error is exponential, that is, the error decays as $O(e^{-\alpha N})$ for some constant $\alpha > 0$.

  An example: a Fourier spectral method applied to linear convection with a smooth initial condition with $N = 16$ already produces an error of 10^{-11}, while a second order accurate finite difference scheme with the same number of unknowns produces an error of 10^{-1} and a fourth order finite difference scheme is barely better at the error level of 10^{-2}.

- High order accurate compact schemes, which can give "spectral-like" resolution for many wave problems, are also popular for solving PDEs with smooth solutions.
- If the computational domain is not a box, then the spectral element method, which combines the advantages of the spectral method in its high order accuracy and the finite element method in its flexibility for arbitrary geometry, would be a good choice.

  The discontinuous Galerkin method, because of its flexibility in meshes, adaptivity, and parallel implementation, is also a good choice.

If the solution of the PDE has discontinuities or sharp gradient regions:

- High order methods (spectral, compact scheme, etc.) with filtering. The filtering can be linear or nonlinear.
  - Advantages: Simple to code: the base algorithm and the filtering can be coded separately and applied sequentially.
  - Disadvantages: Usually there are parameters in the filtering to be tuned. If not tuned well, the result could be either too dissipative or too oscillatory.

- High order WENO finite difference scheme.
  - Advantages: Robust, no user-tuned parameters. Very stable for strong shocks. The code for multi-dimensions is essentially the same as the one for one dimension.
  - Disadvantages: Can only be used on rectangular uniform meshes or smooth curvilinear meshes (to have both conservation and at least third order accuracy). Needs local characteristic decomposition to avoid oscillations during wave interactions. The CPU cost is 4 to 10 times that of a second order scheme depending on the specific equation and implementation.

An example where the solution contains both discontinuities and rich structures in smooth regions: This is the problem of a strong shock interacting with a pair of vortices (Zhang, Zhang and Shu, Physics of Fluids 2006), simulated by the fifth order finite difference WENO scheme on the compressible Navier-Stokes equations. In Figure 1 we plot the shadowgraphs (contours of $\nabla^2 \rho$ where ρ is the density) of an oblique Mach 1.2 shock with a strong colliding vortex pair. We can see clearly that complicated flow structure from the shock vortex interaction is resolved well by the fifth order WENO scheme.

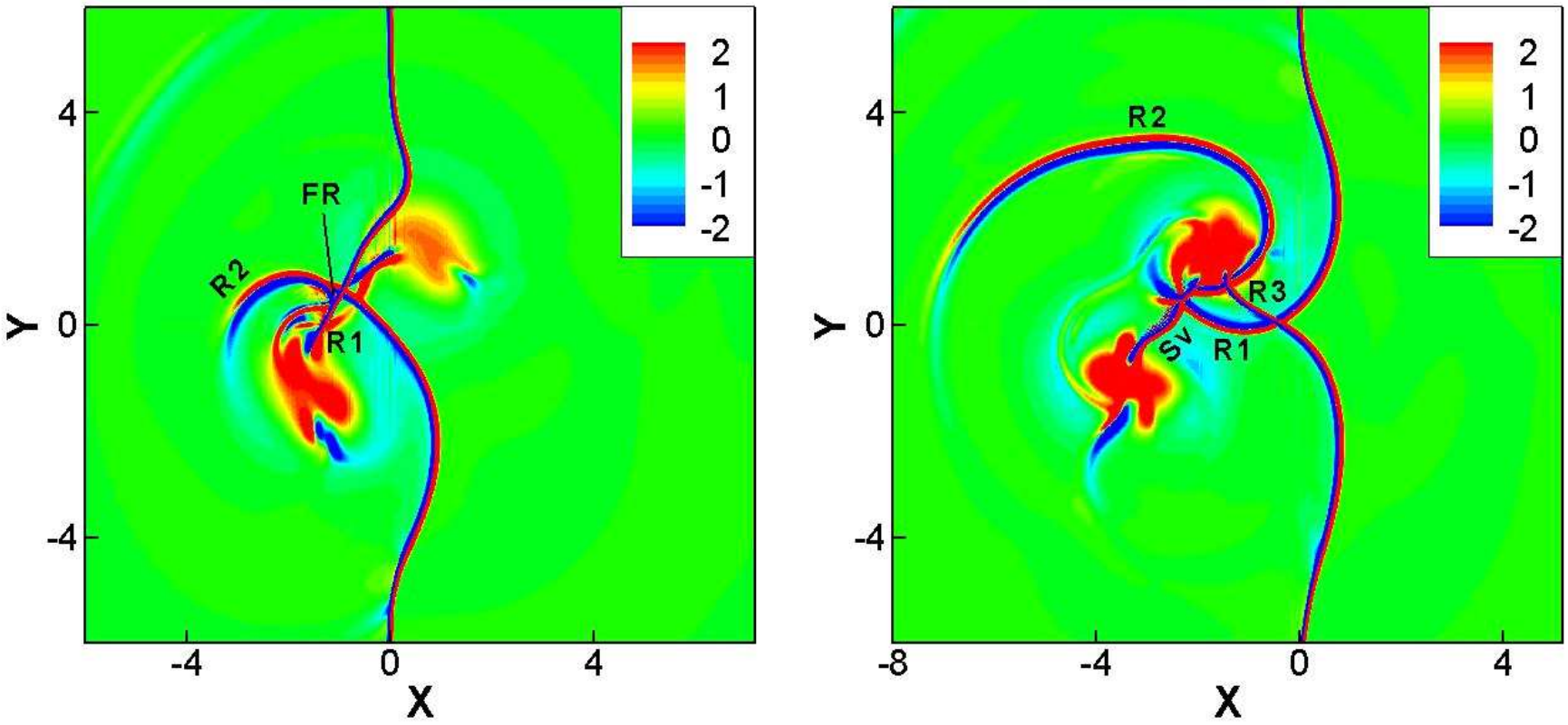

(a) $t = 5.0$ (b) $t = 7.0$

Figure 1: Fifth order WENO simulation of the evolution of an oblique shock and a colliding vortex pair interaction. Shock Mach number $M_s = 1.2$, vortex Mach number $M_\nu = 0.8$, and angle of the oblique shock wave $\alpha = 45°$.

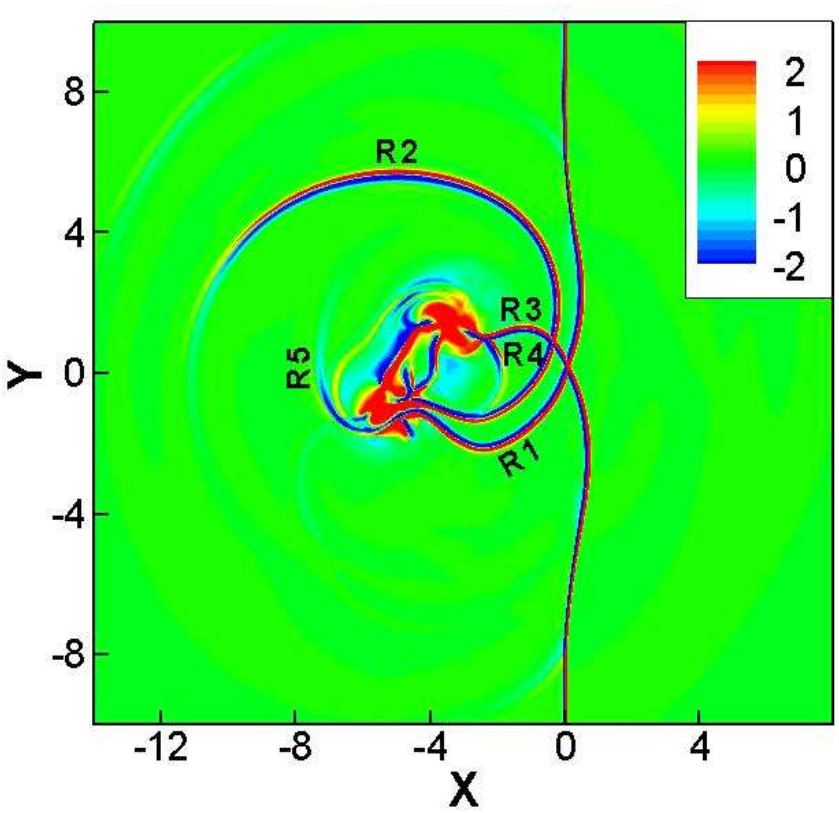

(c) $t = 9.0$

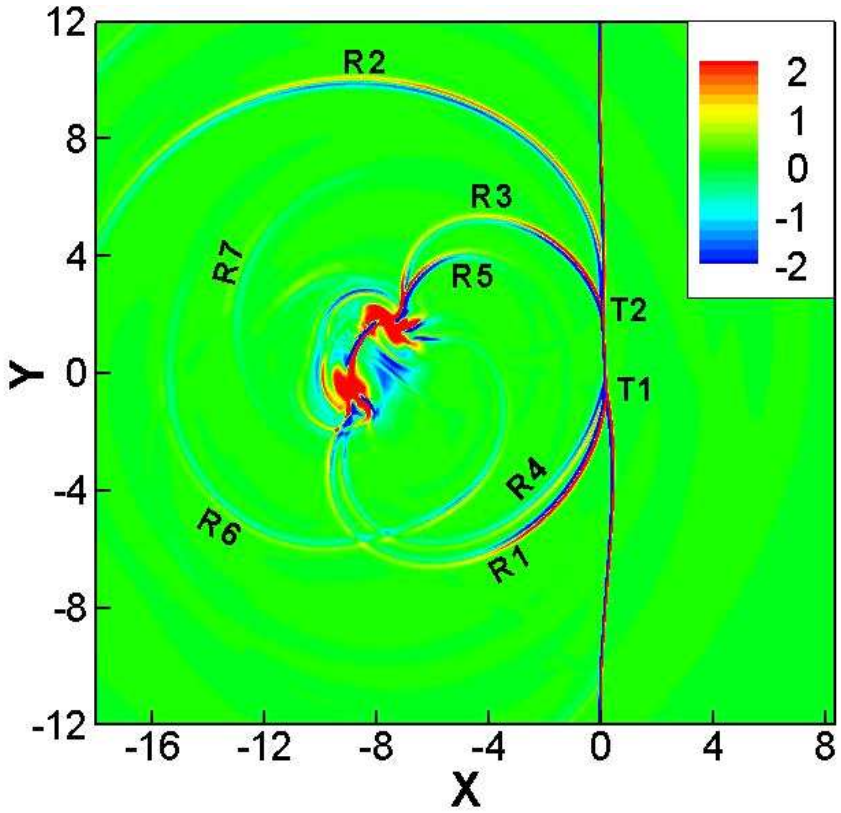

(d) $t = 13.0$

Figure 2: Continued.

- High order WENO finite volume scheme.
  - Advantages: Robust, no user-tuned parameters. Very stable for strong shocks. Can be applied to non-smooth meshes and arbitrary triangulations. The code for multi-dimensional tensor product meshes (do not need to be smooth) is similar as the one for one dimension.
  - Disadvantages: Very expensive for multi-dimensional calculation. It is up to 4 times more expensive than a finite difference WENO scheme on the same mesh with the same order of accuracy for 2D, and up to 9 times for 3D. The algorithm formulation and coding are both very complicated for arbitrary (not tensor product) triangulation.

- Discontinuous Galerkin finite element method.
  - Advantages: Applies to very general geometry, triangulation and boundary conditions. Easy for adaptive computation and parallel implementation. Very good wave resolution capability. Can simulate solutions with strong shocks when suitable limiters are used. Much more theoretical stability results available than finite difference and finite volume WENO schemes.
  - Disadvantages: Coding more complicated than finite difference schemes. Limiters to control oscillations not as robust as the WENO methodology (however recently WENO limiters have been designed by Qiu and Shu). Computer memory is a problem for 3D computation.

An example to show the excellent wave resolution capability of the DG method: we solve the linear convection equation

$$u_t + u_x = 0, \qquad or \qquad u_t + u_x + u_y = 0,$$

on the domain $(0, 2\pi) \times (0, T)$ or $(0, 2\pi)^2 \times (0, T)$ with the characteristic function of the interval $(\frac{\pi}{2}, \frac{3\pi}{2})$ or the square $(\frac{\pi}{2}, \frac{3\pi}{2})^2$ as initial condition and periodic boundary conditions.

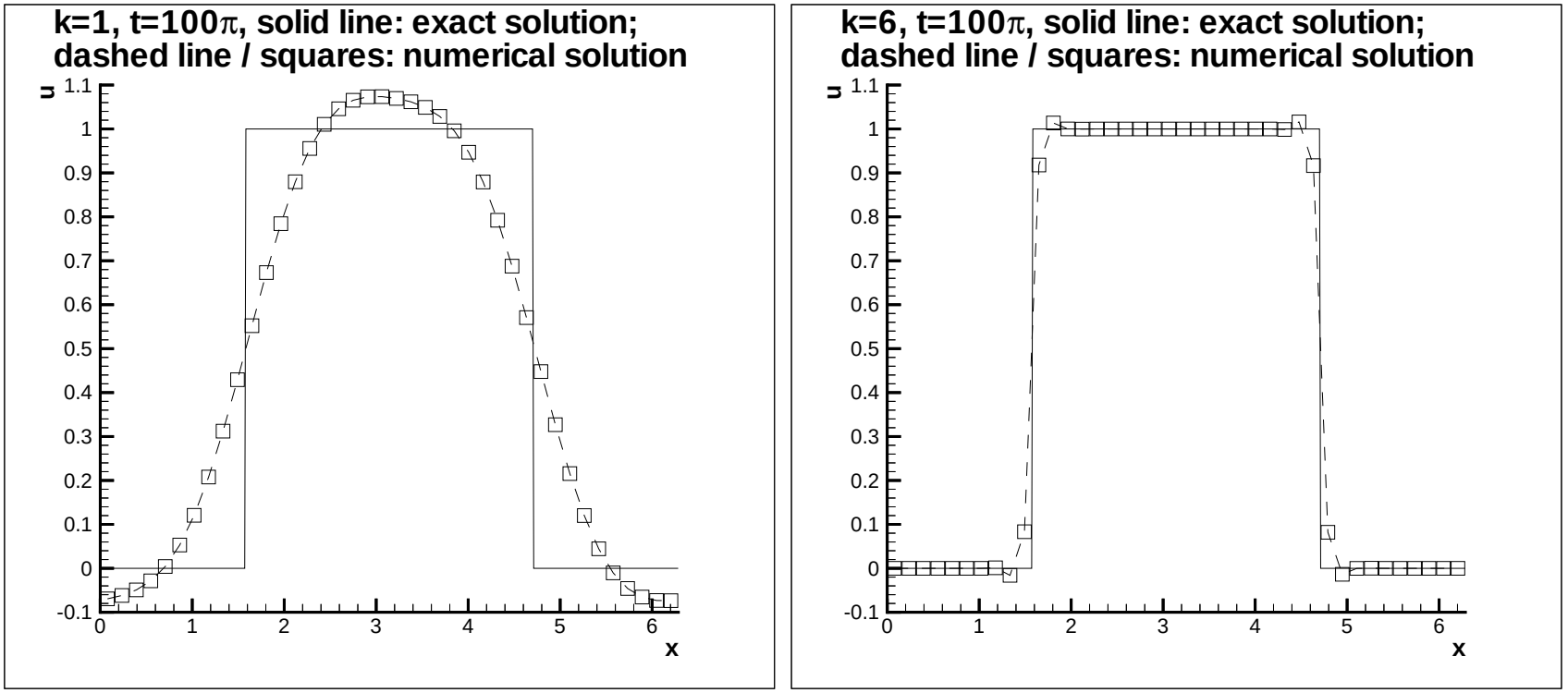

Figure 3: Transport equation: Comparison of the exact and the RKDG solutions at $T = 100\pi$ with second order (P^1, left) and seventh order (P^6, right) RKDG methods. One dimensional results with 40 cells, exact solution (solid line) and numerical solution (dashed line and symbols, one point per cell)

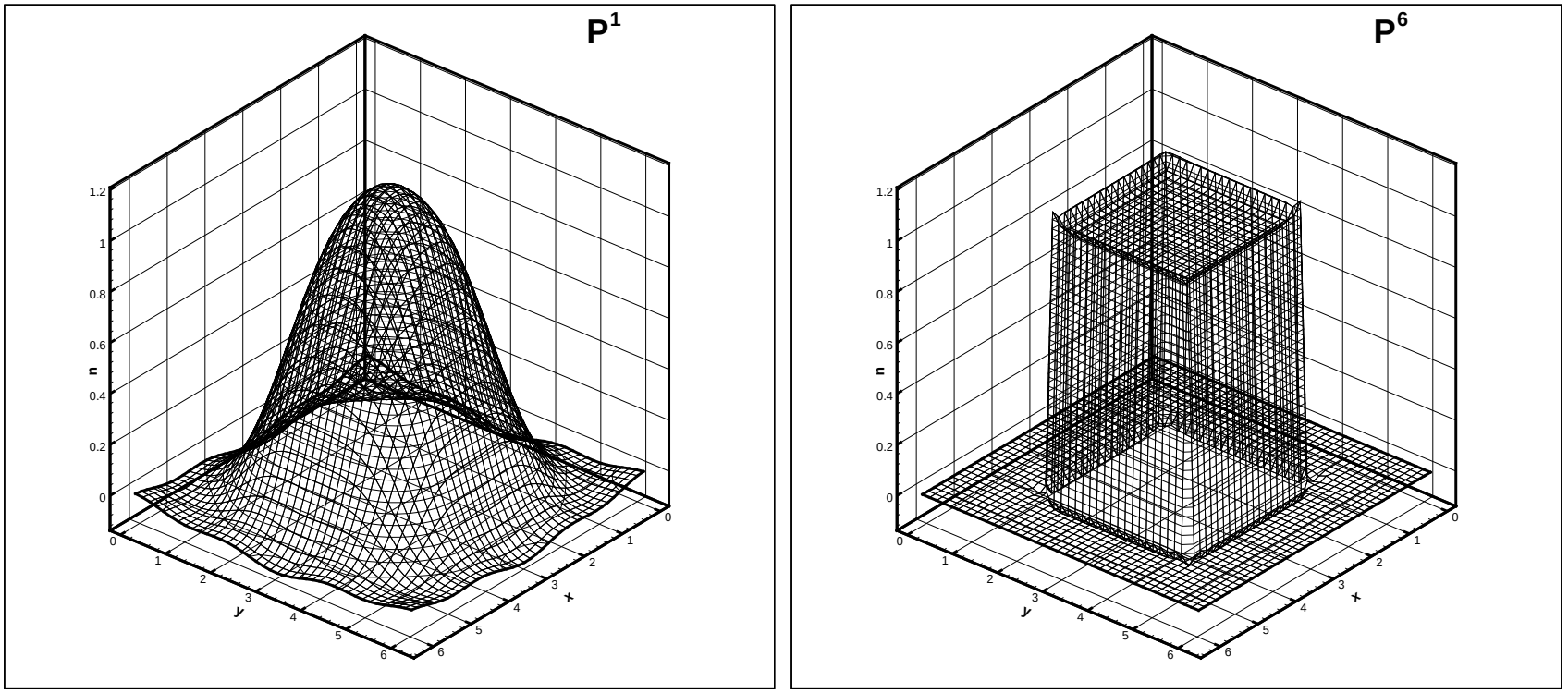

Figure 4: Transport equation: Comparison of the exact and the RKDG solutions at $T = 100\pi$ with second order (P^1, left) and seventh order (P^6, right) RKDG methods. Two dimensional results with 40×40 cells.

For nonlinear problems with shocks: an example is the double Mach reflection problem for the two dimensional compressible Euler equations.

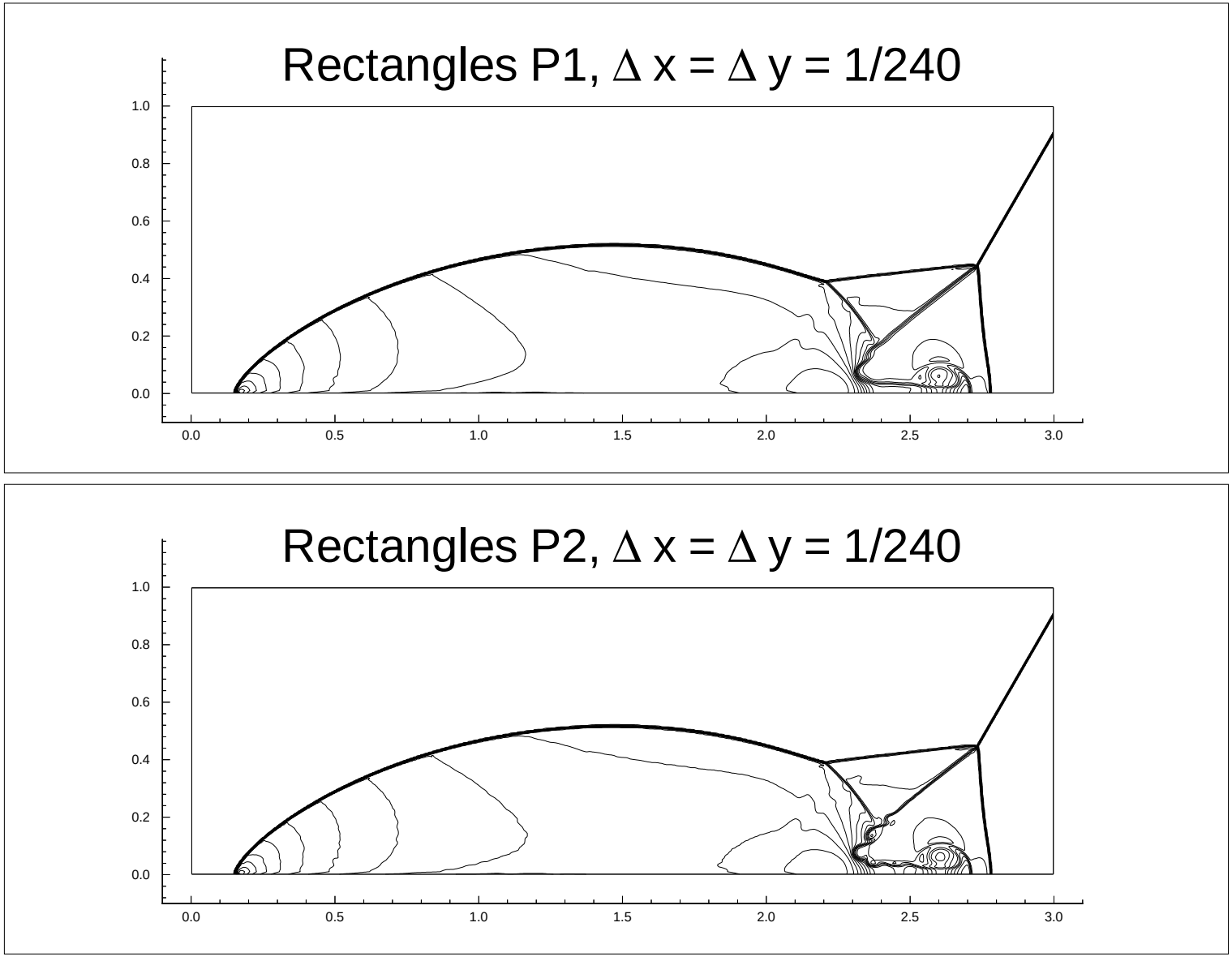

Figure 5: Double Mach reflection. $\Delta x = \Delta y = \frac{1}{240}$. Top: P^1; bottom: P^2.

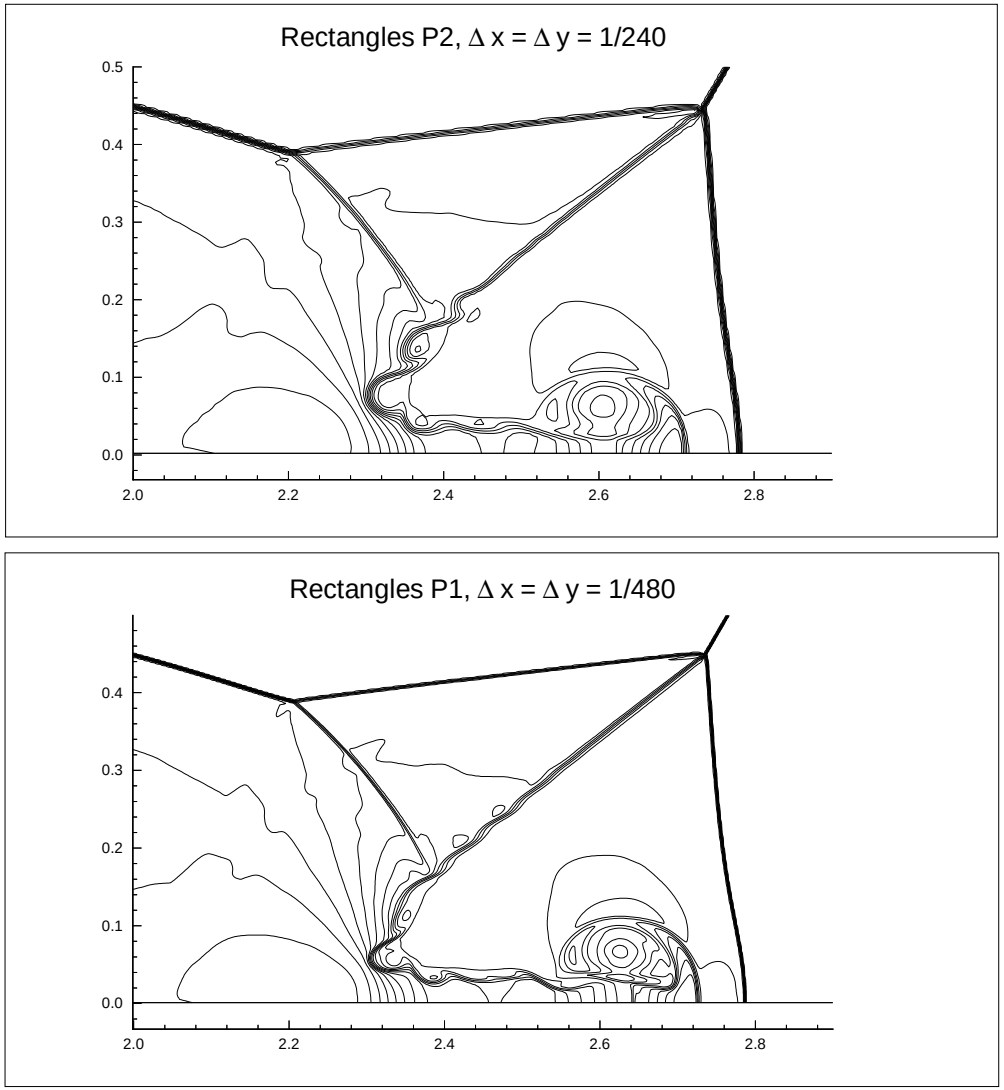

Figure 6: Double Mach reflection. Zoomed-in region. Top: P^2 with $\Delta x = \Delta y = \frac{1}{240}$; bottom: P^1 with $\Delta x = \Delta y = \frac{1}{480}$.

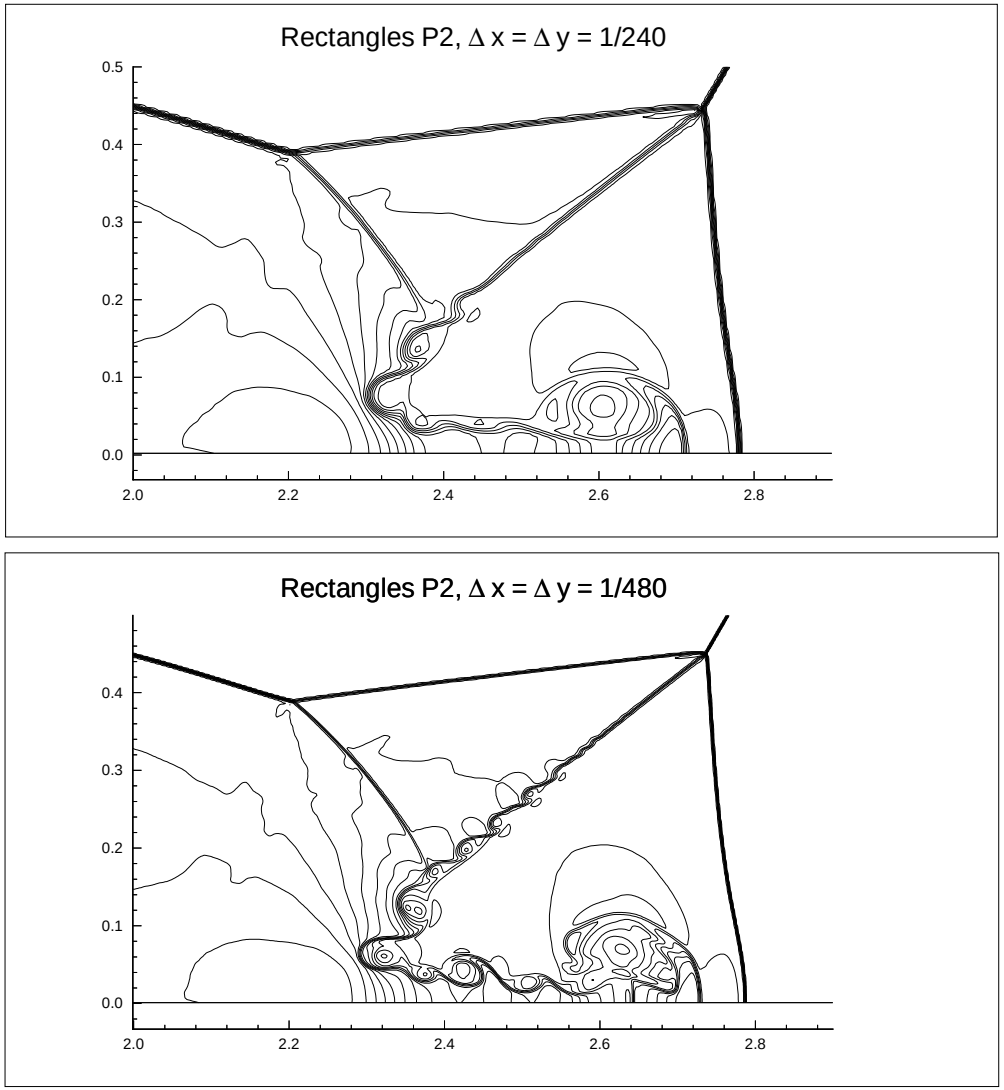

Figure 7: Double Mach reflection. Zoomed-in region. P^2 elements. Top: $\Delta x = \Delta y = \frac{1}{240}$; bottom: $\Delta x = \Delta y = \frac{1}{480}$.

A final example is the flow past a forward-facing step problem for the two dimensional compressible Euler equations. No special treatment is performed near the corner singularity.

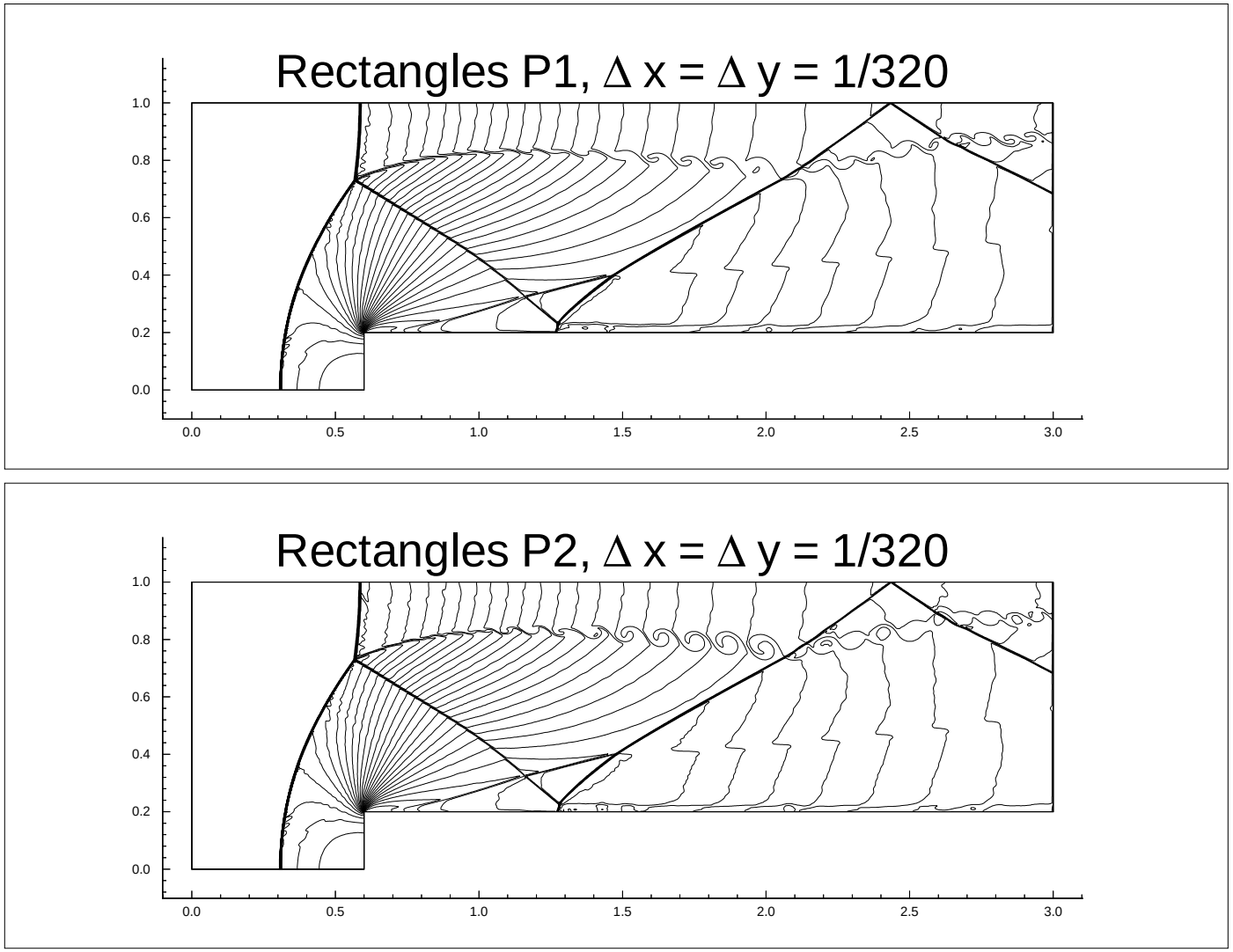

Figure 8: Forward facing step. Zoomed-in region. $\Delta x = \Delta y = \frac{1}{320}$. Left: P^1 elements; right: P^2 elements.

Examples of a few recent developments on high order methods

For WENO schemes:

- High order weighted compact schemes (Zhang and Shu, JCP to appear)
  - Combines the compact schemes and WENO finite difference schemes.
  - Based on weighted interpolation of fluxes, the main subroutine similar to finite difference WENO schemes.
  - Similar to finite difference WENO scheme in shock resolution, better dissipation and dispersion error control than finite difference WENO scheme of the same order of accuracy.

- Towards direct numerical simulation of compressible turbulence.

An example: Rayleigh-Taylor instability. It happens on an interface between fluids with different densities when an acceleration is directed from the heavy fluid to the light one. The instability has a fingering nature, with bubbles of light fluid rising into the ambient heavy fluid and spikes of heavy falling into the light fluid.

We can observe that the weighted compact schemes can produce more small vortices in the shear layer than the regular finite difference WENO scheme, indicating that the weighted compact schemes have better resolution to capture small scale structures.

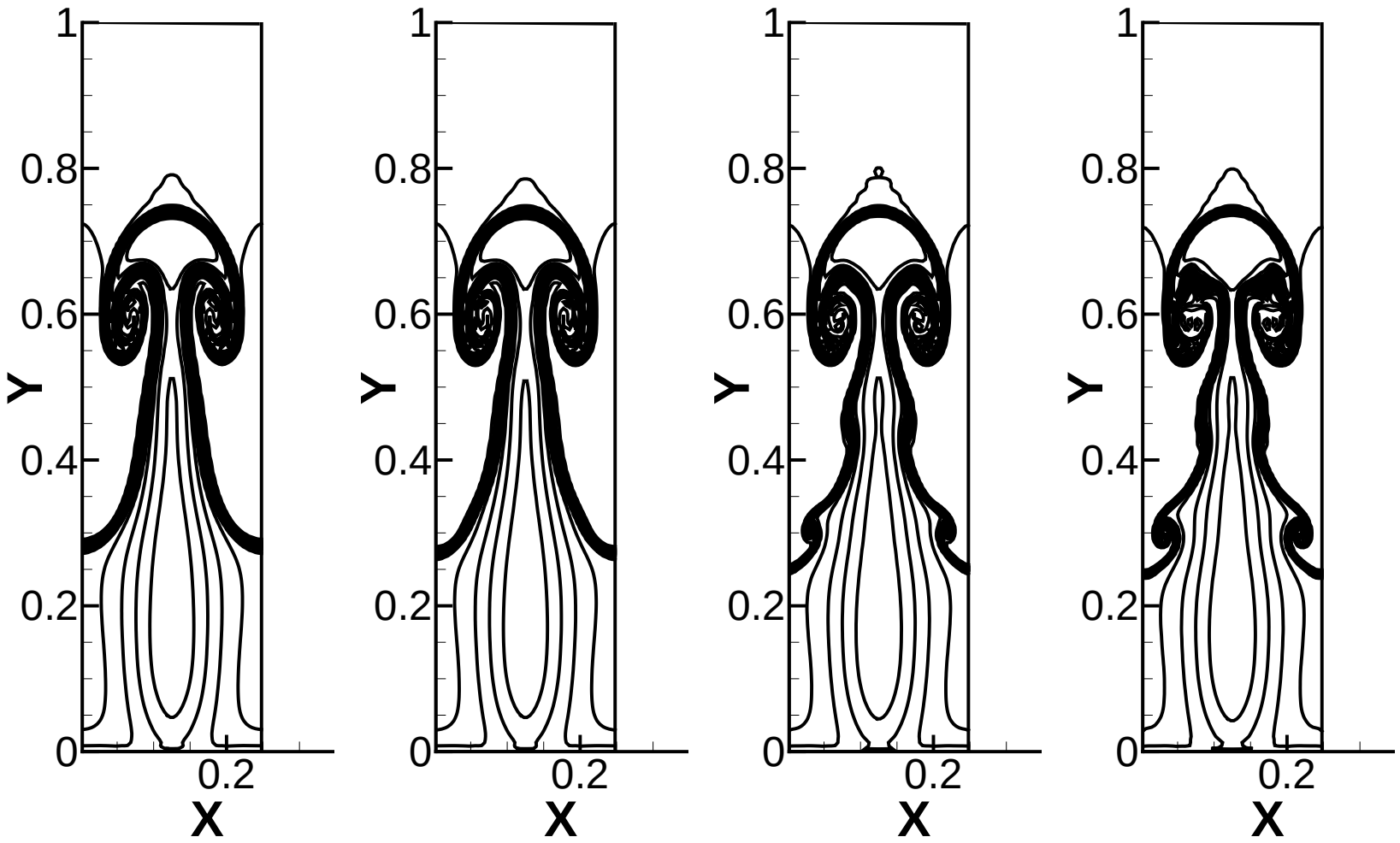

(a) (Left to right) WENO5; WCOMP4; WCOMP6; WCOMP8. $\Delta x = \Delta y = \frac{1}{240}$

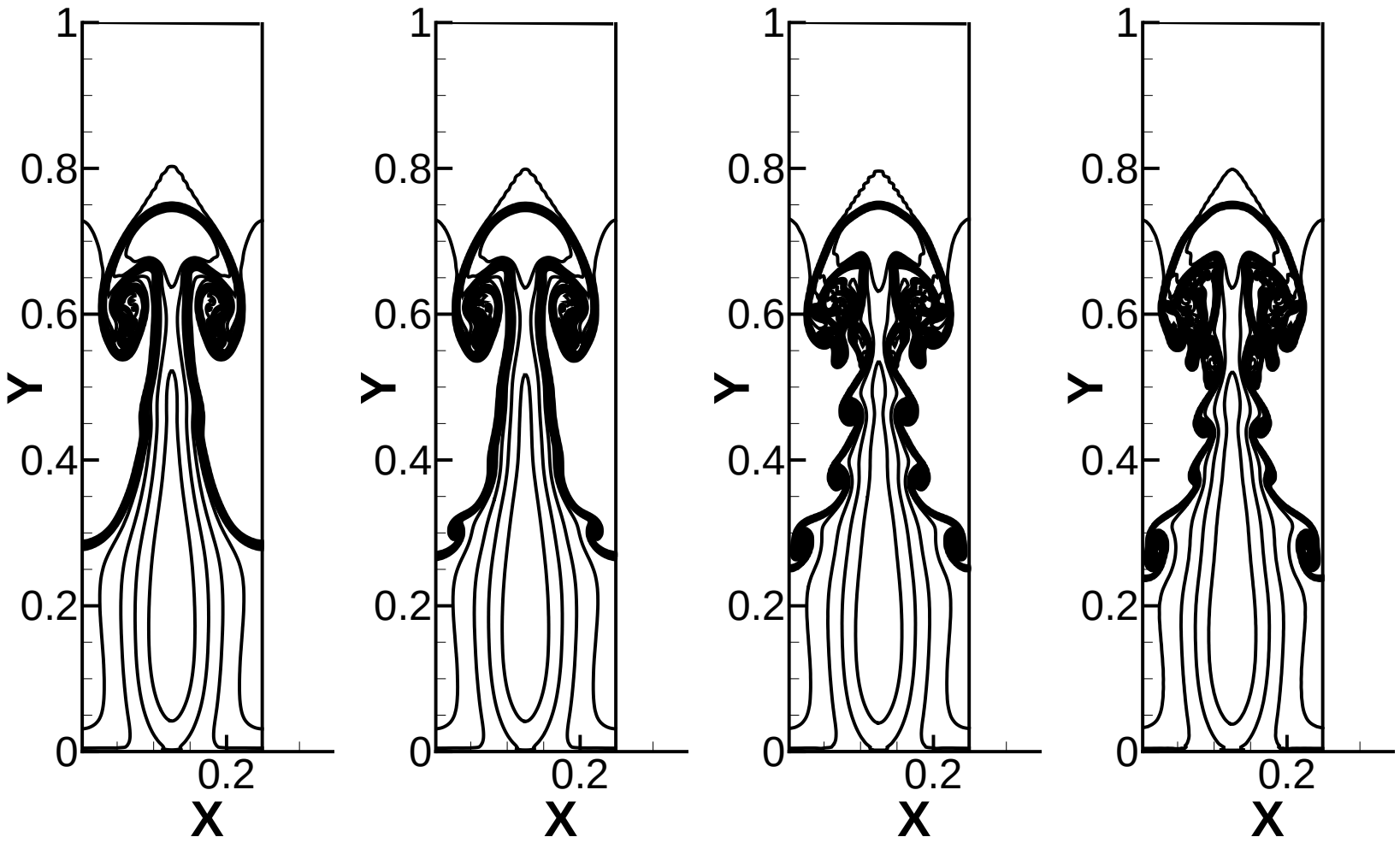

(b) (Left to right) WENO5; WCOMP4; WCOMP6; WCOMP8. $\Delta x = \Delta y = \frac{1}{480}$

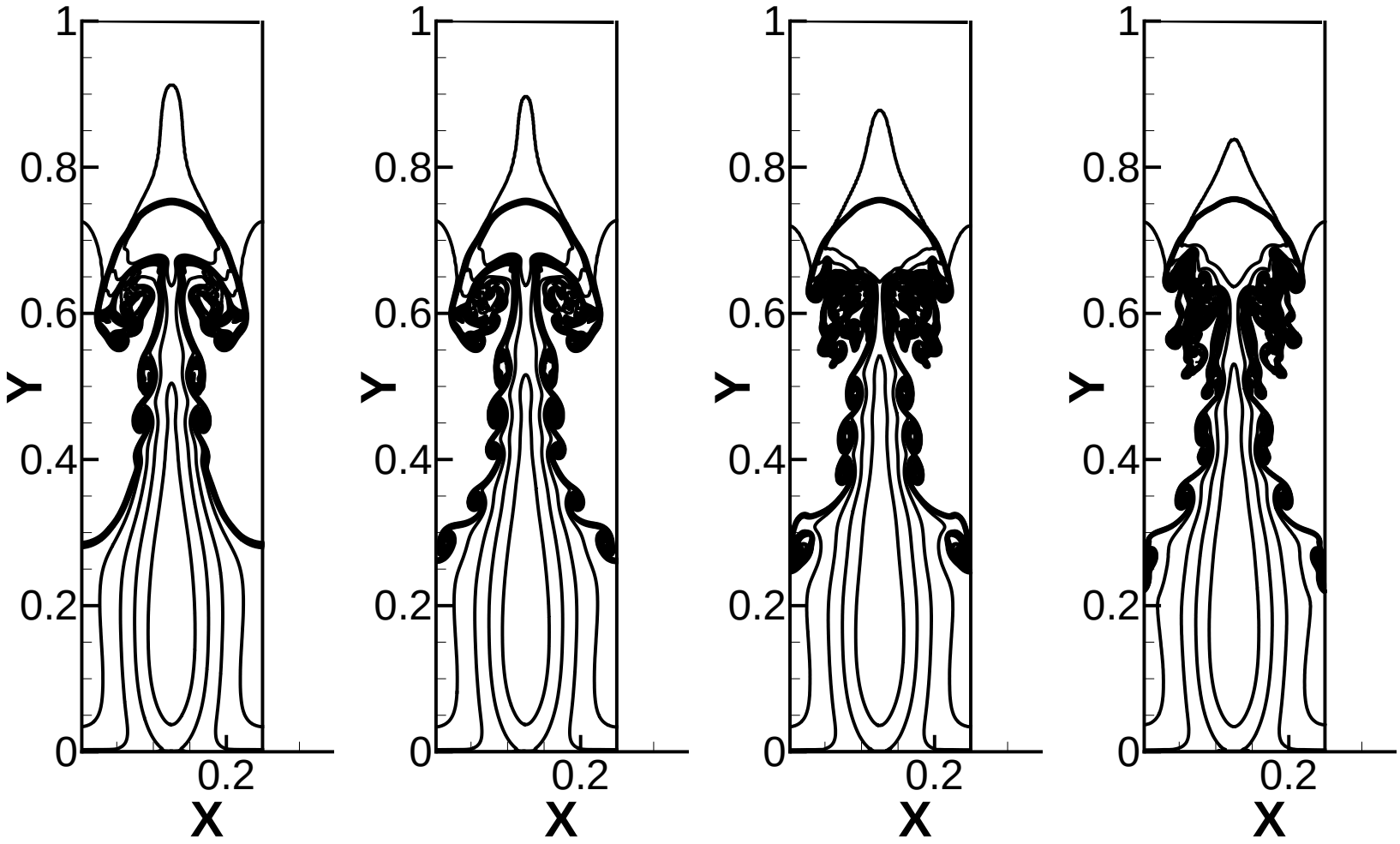

(c) (Left to right) WENO5; WCOMP4; WCOMP6; WCOMP8. $\Delta x = \Delta y = \frac{1}{960}$

Figure 9: Rayleigh-Taylor Instability. Density ρ; 15 equally spaced contour lines from $\rho = 0.952269$ to $\rho = 2.14589$.

- Well balanced WENO schemes (Xing and Shu, JCP 05; JSC 06; JCP 06; CiCP 06; Noelle, Xing and Shu, JCP 07).
  - A hyperbolic balance law (conservation law with source term)

$$u_t + f(u,x)_x = g(u,x) \tag{2}$$

    admits steady state solutions in which the source term $g(u,x)$ is exactly balanced by the flux gradient $f(u,x)_x$. The objective of well balanced schemes is to preserve exactly some of these steady state solutions.
  - This is a non-trivial task because such steady state solutions are usually not polynomials or other simple functions and their explicit formulas are of course unknown.

- Most schemes would therefore only be able to resolve such steady states to the level of truncation errors of the schemes. But a well balanced scheme aims at resolving such steady states exactly, up only to round-off errors.
- The main reason that such well balanced schemes might be of interest is that often we have physical applications of a solution which is *very close to* the relevant steady state, i.e. a small perturbation from the steady state, and we are interested in resolving such small perturbations.
- Until recently, most well balanced schemes are only at most second order accurate. We have developed a general framework via source term splitting to design high order WENO and DG well balanced schemes.

We will demonstrate the advantage of a well balanced scheme through some figures. We can see from Figure 10, which is the solution of a well balanced WENO scheme for a shallow water equation with moving water, that the very small perturbation (which can be hardly observed in the original picture without zooming) is captured well without spurious oscillations by a relatively coarse mesh of 200 points. For this example, if we use a non well-balanced WENO scheme with the same number of mesh points, we will not be able to resolve the small bumps at all.

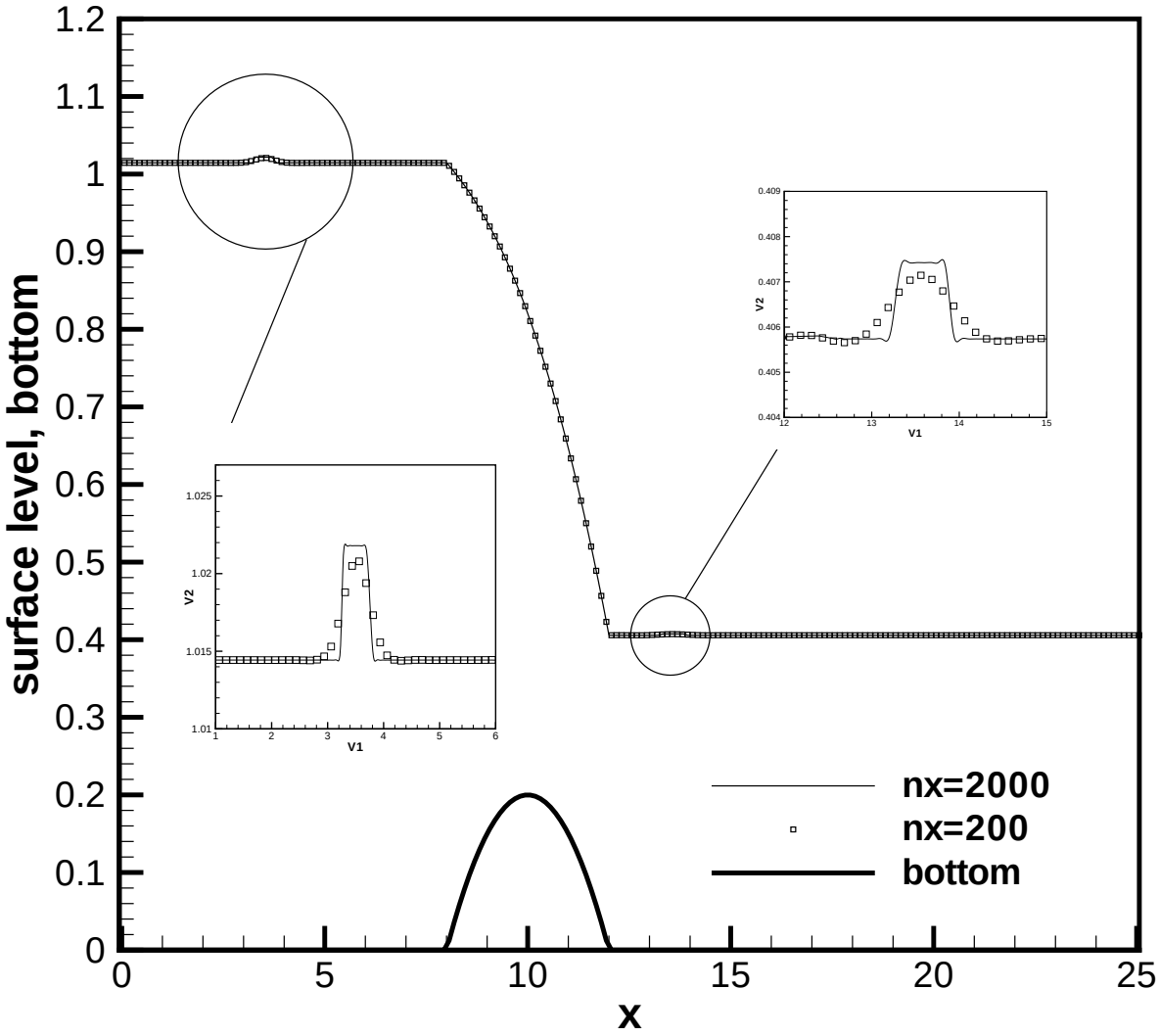

Figure 10: Small perturbation of the transcritical flow.

In Figure 11, which is a two dimensional simulation, we can clearly see that the result of the high order well balanced WENO scheme (left) is very clean, while that of the non well-balanced WENO scheme has “large” spurious waves at this grid resolution. Of course, if we refine the mesh sufficiently, these spurious waves will diminish and eventually disappear (to visual observation), as they are at the level of truncation errors which will decay with a refinement of the mesh.

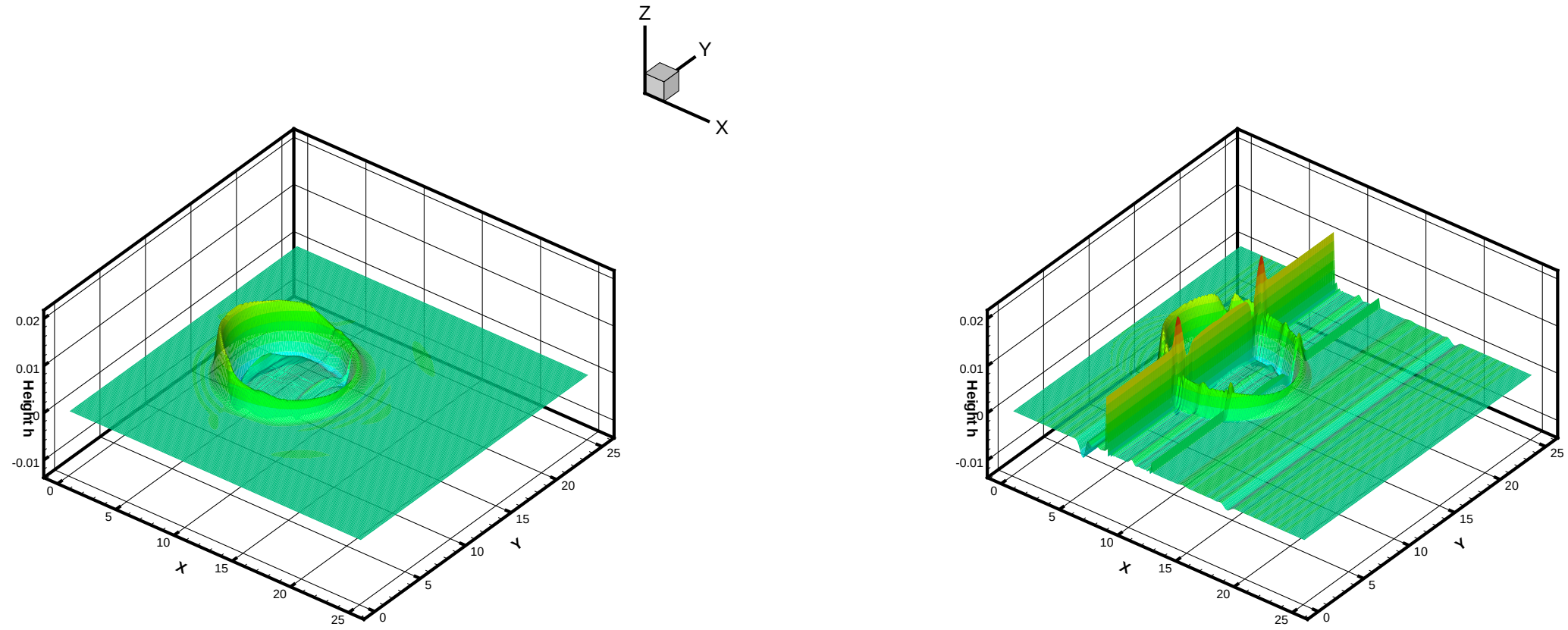

Figure 11: Water height. 200×200 uniform mesh for the shallow water equation. Left: results based on the well balanced WENO scheme. Right: results based on the non well-balanced WENO scheme.

- WENO schemes for kinetic and Boltzmann type equations (Carrillo, Gamba, Majorana and Shu, JCP 03 and 06; Qiu, Shu, Fang et al. New Astronomy 07 and 08; Astrophysical J. 07).
  - Kinetic and Boltzmann type equations are usually scalar equations for the evolution of a (unscaled) probability density function, which is a convection equation with a collision source term.
  - The convective nature of these equations makes the usual linear schemes subject to numerical oscillations and instability, especially when the meshes are coarse and hence there are “sharp transitions” (on the mesh level) in the numerical solution.
  - The dimension of the kinetic and Boltzmann type equations is usually very high: in the most general case it is 6D + time. We can now solve 5D + time. Only a coarse mesh can be afforded.

Our WENO solver is stable and quite accurate on coarse meshes.

For example, in the MOSFET simulation (in semiconductor device simulations) shown in Figure 12, our WENO solver, using a mesh of $49 \times 33 \times 66 \times 12 \times 12$ grid points can produce very accurate results comparing well with the benchmark DSMC data (the oscillatory curves in the figure).

The simulation of this five dimensional plus time problem took about 3 days on a standard PC, indicating that our WENO solver is quite efficient. A parallel implementation of this solver is also worked out and used to compute larger problems.

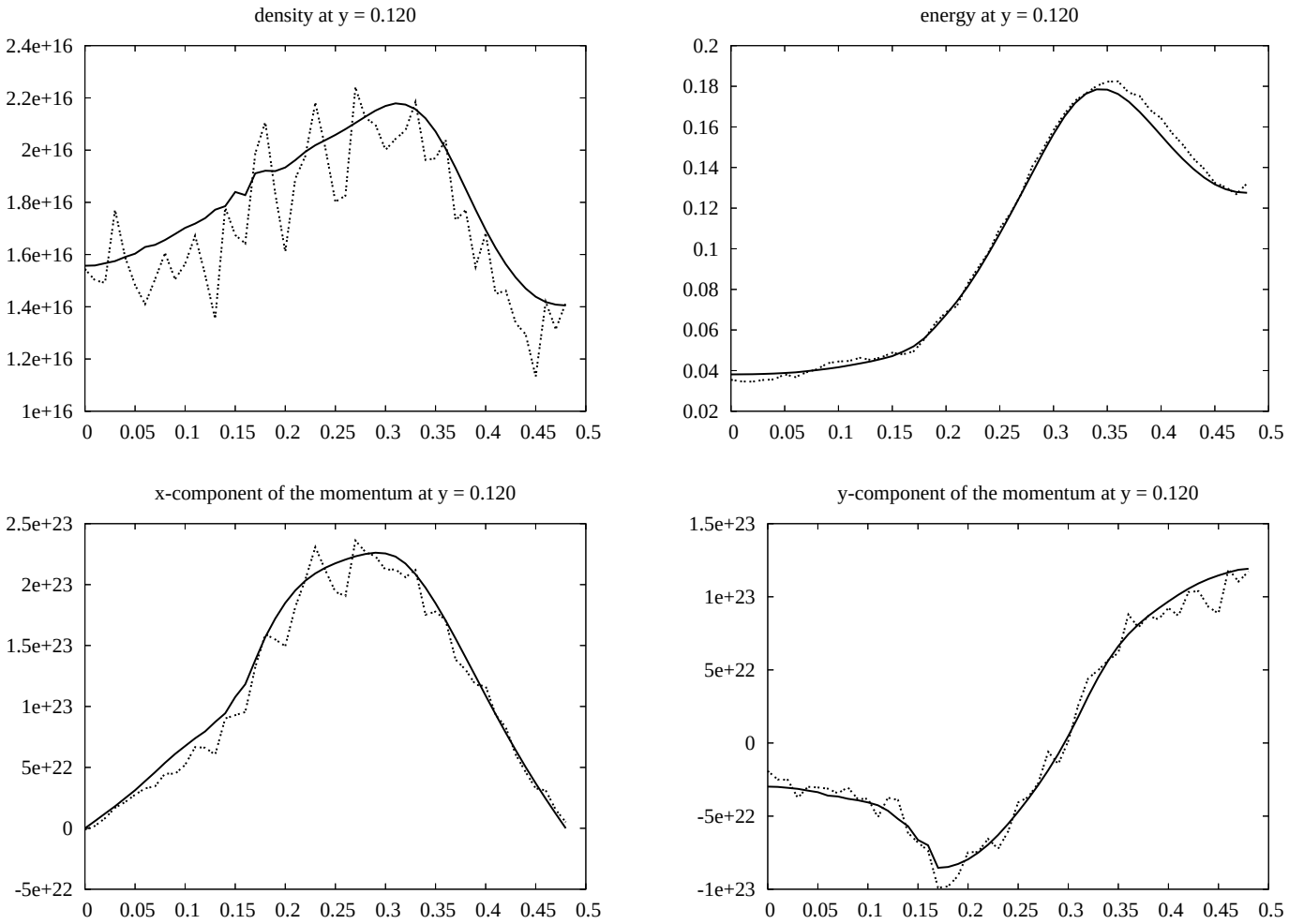

Figure 12: MOSFET device. WENO Boltzmann versus DSMC at $t = 5$ ps and $y = 0.12$.

- High order ENO conservative Lagrangian type schemes for the compressible Euler equations (Cheng and Shu, JCP 07; CiCP to appear).
  - Based on conservative ENO reconstructions over quadrilateral meshes (second order) or over curved quadrilateral meshes with quadratic curve boundaries (third order).
  - The scheme is conservative and demonstrates the designed second and third order accuracy in two dimensions.
  - The advantage of Lagrangian type schemes is that they resolve material interfaces (contact discontinuities) more sharply than Eulerian type schemes.

For DG schemes:

- DG method for solving nonlinear high order PDEs.
  - Local DG (LDG) methods for nonlinear PDEs containing higher order spatial derivatives.
  - A careful design of numerical fluxes is the key for the success of the resulting LDG scheme. Patterns do exist.
  - Typical theoretical results include a nonlinear stability of the numerical solution either in the L^2 norm or in a physically relevant energy. This stability is valid regardless of the regularity of the solution. Error estimates can also be obtained for smooth solutions.

- Recent results include the design and analysis of LDG schemes for the following nonlinear PDEs:
  - Cahn-Hilliard type equations (Xia, Xu and Shu, JCP 07);
  - Allen-Cahn/Cahn-Hilliard system (Xia, Xu and Shu, CiCP to appear);
  - Camassa-Holm equation (Xu and Shu, SINUM 08);
  - Hunter-Saxton equation (Xu and Shu, SISC submitted);
  - Surface diffusion and Willmore flow of graphs (Xu and Shu, JSC submitted).

Example: We solve the Cahn-Hilliard equation with an initial condition which is a random perturbation of uniform state $u = 0.63$ with a fluctuation no larger than 0.05. We use the P^1 elements on a uniform mesh with 80×80 cells. The concentration evolution can be categorized in two stages. The first stage is governed by spinodal decomposition and phase separation (the first four figures in Fig. 13). The second stage is governed by grain coarsening (from $t = 8 \times 10^{-6}$ onwards).

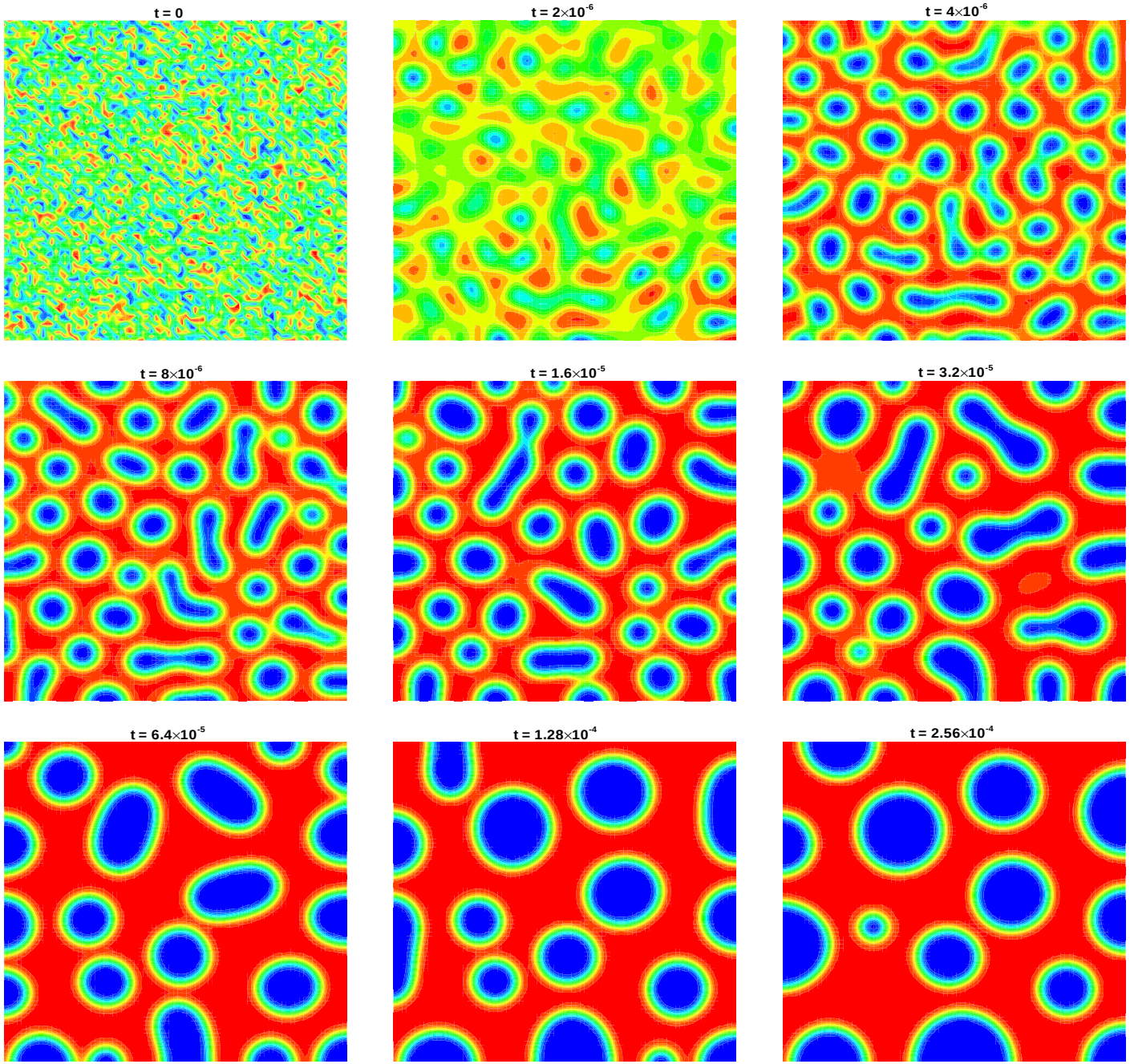
t = 0
t = 2×10^-6
t = 4×10^-6
t = 8×10^-6
t = 1.6×10^-5
t = 3.2×10^-5
t = 6.4×10^-5
t = 1.28×10^-4
t = 2.56×10^-4

- Multiscale solvers based on DG schemes.
  - Heterogeneous multiscale method (HMM) + DG
    - Linear hyperbolic and parabolic equations (Chen, E and Shu, SIMMS 05)
    - Nonlinear Euler equations (Chen, E and Shu, SIMMS 05)
    - Dynamics of crystalline solids (Wang, Li and Shu, SIMMS 08)
  - Domain decomposition (Chen, E, Liu and Shu, JCP 07)
    - Euler equations / BGK model
    - Semiconductor devices: hydrodynamic (HD) model / kinetic model

- DG method with multiscale basis
  - Elliptic equations with oscillatory coefficients (Yuan and Shu, IJNME 08)
  - Semiconductor devices: Schrödinger-Poisson system (Wang and Shu, JSC submitted)

We consider the Euler equation of compressible gas dynamics

$$u_t^\varepsilon + f(u^\varepsilon)_x = 0, \tag{3}$$

where $u^\varepsilon = [\rho^\varepsilon, \rho^\varepsilon v^\varepsilon, E^\varepsilon]^T$,
$f(u^\varepsilon) = [\rho^\varepsilon v^\varepsilon, \rho^\varepsilon (v^\varepsilon)^2 + p^\varepsilon, v^\varepsilon (E^\varepsilon + p^\varepsilon)]^T$, and

$$p^\varepsilon = a^\varepsilon(x)[(E^\varepsilon - \frac{1}{2}\rho^\varepsilon (v^\varepsilon)^2)(\gamma - 1)] \tag{4}$$

where γ is a constant. This is clearly equivalent to having an oscillatory γ

$$\gamma^\varepsilon = 1 + (\gamma - 1)a^\varepsilon(x).$$

In the numerical test, we take

$$a^\varepsilon(x) = \frac{1}{1 + 0.1\sin(\frac{x}{\varepsilon}) + 0.1\sin(x)}. \tag{5}$$

We will use the following notations:

- u^ε: the solution of (3)-(4), with a^ε given by (5);
- $\bar{u}^\varepsilon$: the local average of u^ε, obtained by convolving u^ε with a mass-one local kernel of width $O(\varepsilon)$;
- $\tilde{u}$: the solution of (3)-(4) with $a^\varepsilon(x)$ in (4) replaced by a simple average

$$\tilde{a}(x) = \frac{1}{2\pi}\int_0^{2\pi} \frac{1}{1+0.1\sin(y)+\sin(x)}dy.$$

- $\bar{u} = \lim_{\varepsilon\to 0} \bar{u}^\varepsilon$. This limit will serve as our "exact" solution of the homogenized Euler problem, which is not explicitly known.

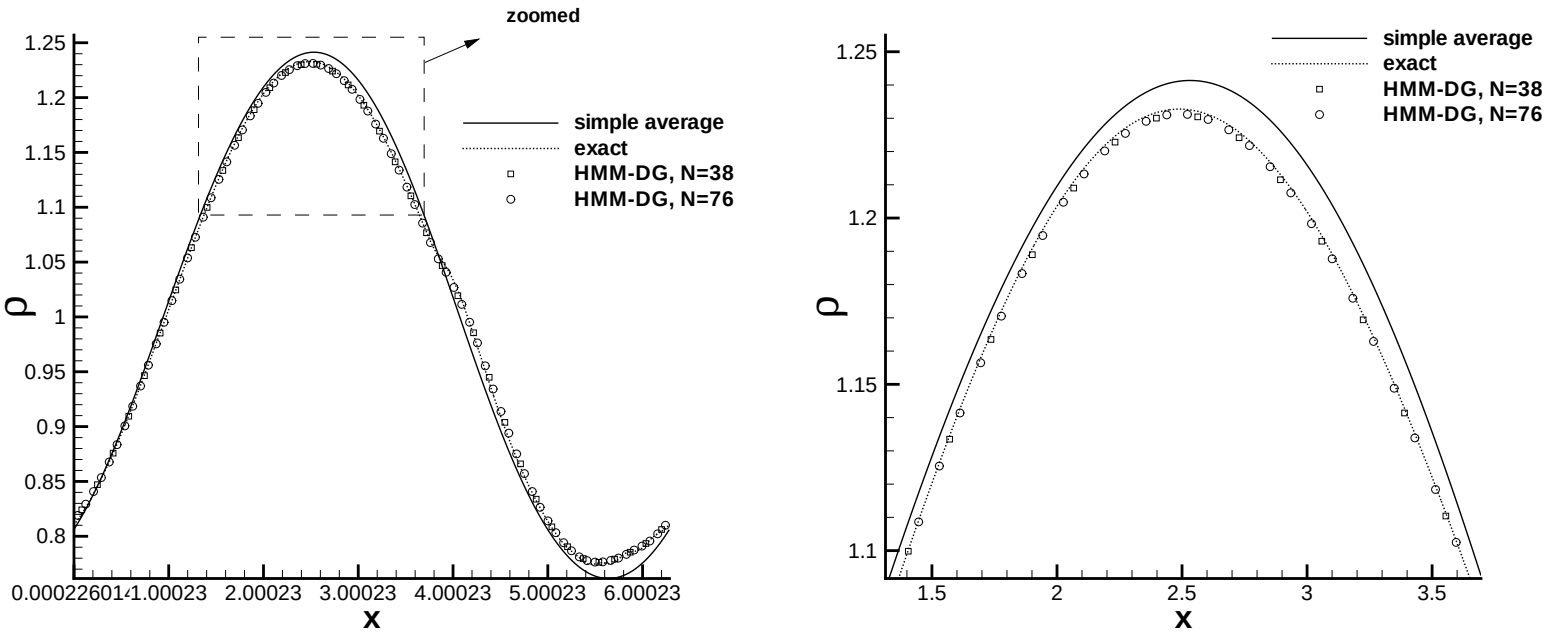

Figure 14: Density ρ. The HMM-DG solution with $N = 38$ and $N = 76$ uniform elements for $\varepsilon = 10^{-6}$, versus the "converged" local average solution $\bar{u}$ to the nonlinear oscillatory Euler equations (denoted by "exact" in the figures). The solution $\tilde{u}$ of the simply averaged Euler equations (denoted by "simple average" in the figures) is also plotted as a reference. Left: the solutions in the whole interval; right: zoomed around $x = 2.5$.

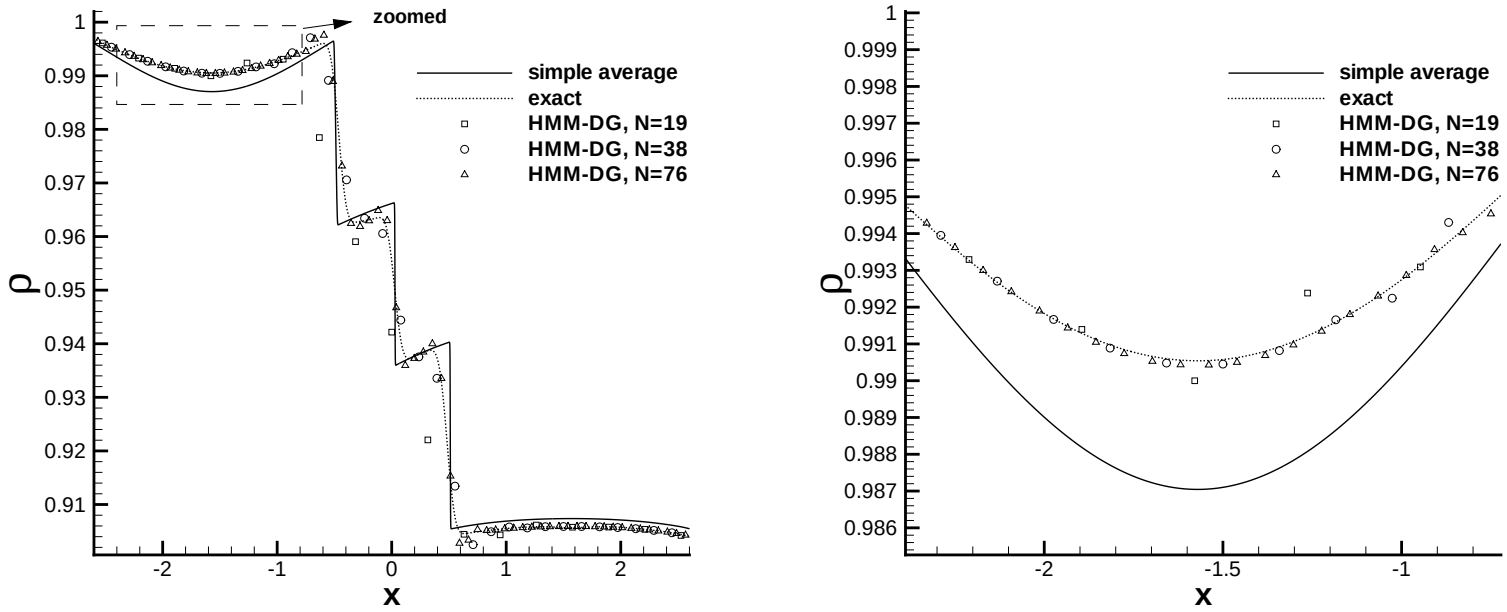

Figure 15: Sod's Shock tube problem. Density ρ. The HMM-DG solution with $N = 19$, 38 and 76 uniform elements for $\varepsilon = 10^{-6}$, versus the converged "exact" locally averaged solution $\bar{u}$ to the nonlinear oscillatory Euler equations. The solution $\tilde{u}$ of the simply averaged Euler equations (simple average) is also plotted as a reference. Left: the solutions in the whole interval; right: zoomed around $x = -1.5$.

- Superconvergence and time evolution of errors.
  - DG approximation to smooth solutions of one and two dimensional conservation laws

$$u_t + f(u)_x = b(x,t), \tag{6}$$

and

$$u_t + f(u)_x + g(u)_y = b(x,y,t). \tag{7}$$

- The error between the DG solution and a particular projection of the exact solution superconverges. For P^k elements this error is typically h^{k+2} (one order higher than usual).
- As a consequence, the error between the DG solution and the exact solution does not grow with time, for a long time period $0 \leq t \leq O(h^{-1})$.
- The conclusion can be proved for linear problems and seems to hold also for nonlinear problems using upwind fluxes.
- The conclusion also holds for convection-diffusion equations.

Table 1: Example. Linear convection with $e^{\sin(x)}$ initial condition. P^3 polynomials, uniform meshes.

		$T = 10$		$T = 100$		$T = 500$	
	N	L^2 error	order	L^2 error	order	L^2error	order
$\bar{e}$	5	5.40E-03	-	2.86E-02	-	6.70E-02	-
	10	8.70E-05	5.96	7.65E-04	5.22	3.24E-03	4.37
	20	1.11E-06	6.30	7.50E-06	6.67	3.71E-05	6.45
	40	2.61E-08	5.40	6.57E-08	6.84	3.04E-07	6.93
e	5	5.50E-03	-	2.89E-02	-	6.70E-02	-
	10	2.09E-04	4.72	7.88E-04	5.19	3.24E-03	4.37
	20	1.22E-05	4.09	1.43E-05	5.79	3.91E-05	6.38
	40	7.65E-07	4.00	7.67E-07	4.22	8.22E-07	5.57

Concluding remarks

- High order methods have a good potential for large scale simulation of complex applications.
- Multiscale, adaptivity, and numerical methods obeying as many physical properties (invariants, asymptotics) would be under intensive research.
- Mathematics can play an essential role in multiscale modeling and algorithms, error indicators for adaptivity, structure-preserving numerical methods, etc.